Electrical Power and Energy Systems 83 (2016) 335–351

Contents lists available at ScienceDirect

Electrical Power and Energy Systems

journal homepage: www.elsevier.com/locate/ijepes

Strategic approach for reinforcement of intermittent renewable energy sources and capacitor bank for sustainable electric power distribution system

Partha Kayal [a,*], C.K. Chanda [b]

[a] Department of Electrical Engineering, Future Institute of Engineering and Management, Kolkata 700150, India
[b] Department of Electrical Engineering, Indian Institute of Engineering Science and Technology, Shibpur, Howrah 711103, India

ARTICLE INFO

Article history:
Received 5 September 2015
Received in revised form 4 April 2016
Accepted 8 April 2016

Keywords:
Renewable energy resources
Optimization
Load growth
Distribution network

ABSTRACT

To meet ever increasing load demand in a sustainable way, reinforcement of photovoltaic (PV) array, wind turbine (WT) and capacitor bank in distribution network is proposed in this paper. A comprehensive planning model is presented to determine location and required installation capacity of multiple PV array, WT and capacitor units in an electric power distribution network under heavy load growth situation. Intermittent power generation of renewable energy sources (RESs) are quantified with suitable probability distribution functions and incorporated in the planning model. The planning approach considers several welfare areas in the distribution systems, viz., increment of profit margin, reduction of carbon-di-oxide emission, minimization of distribution power losses, enhancement of voltage stability level and improvement of the network security considering power flow, voltage limit, line capacity, RES penetration, capacitor penetration and utility economy constraint. Non-dominated sorting based multi-objective particle swarm optimization algorithm along with fuzzy decision making criteria is used to find the best allocation alternative for mix RES and capacitor planning problem. The effectiveness of the proposed model has been tested on a typical 28-bus Indian rural distribution network. The results show that more efficient techno-eco-environmental optimization can be obtained from combined RES and capacitor planning model.

Introduction

Power utilities around the world are faced with great challenges to keep up to the increasing demand of electric power. Global warming threat, dwindling resources of fossil fuels, economic and infrastructural constraints to build new power plants, and limited transmission and distribution corridors are driving the utilities to seek alternative methods to meet the increased demand. Solar and wind energy are the two most viable and environmental friendly RESs which have attracted the attention of utilities worldwide [1]. Unlike centralized bulk power stations RESs are small scale power generation units and can be directly installed in a distribution network. However, a common drawback of solar and wind power generation is their unpredictable nature and high dependency on weather conditions. The problems can be partially overcome utilizing the two resources in a proper combination as they are usually complementary in nature [2,3]. The application of two different RESs together in the network increases the complexity and makes such hybrid systems more difficult to analyze. Planning of distribution network with only RESs is not very fruitful because of high implementation cost and limited reactive power support. So, reinforcement of combined RES and capacitor could be an attractive option for proper design and exploitation of distribution network. The parallel use of capacitor bank improves power quality parameters by injecting the reactive power into the network with low expense. Moreover, proper allocation of RESs and capacitor banks in the distribution network defers major system upgrade, reduces overall energy loss and improves reliability. However, connection of new facilities in the network is not a simple plug and play problem. Sitting and sizing of PV arrays and wind turbines (WTs) along with shunt capacitors need to be investigated carefully to avoid voltage rise and line over loading problems. The planning of RESs and capacitors in the distribution network should be modelled in the form of an optimization problem to get maximum benefit.

* Corresponding author.
E-mail addresses: partha_kayal@yahoo.co.in (P. Kayal), ckc_math@yahoo.com (C.K. Chanda).

http://dx.doi.org/10.1016/j.ijepes.2016.04.029
0142-0615/

Although numbers of paper have appeared on sizing optimization of autonomous hybrid solar–wind system very less effort was devoted towards grid interactive renewable energy system design. In Refs. [4,5,7–10], the authors have focused on planning of RESs considering different technical, economic and environmental prospects. PV array, WT and storage battery were used for optimum design of a hybrid system considering cost, reliability and emission in Ref. [4]. Bayod-Rujula et al. [5] have analyzed the interaction of hybrid PV–Wind systems plus batteries with the utility network and tried to find the best combination of the RESs and the size of the battery. However, it has been observed that configuration without battery storage is more graceful for social, economic and environmental sustainability [6]. In Ref. [7], the authors have utilized multi-objective artificial bee colony (MOABC) algorithm to determine the capacity of hybrid PV/WT/FC energy system and the open tie switch numbers. The objectives considered for the optimization were power loss minimization, voltage stability maximization, cost reduction of energy generated and total emission. Khatod et al. [8] have proposed an evolutionary programming based approach to find optimum locations of PV arrays and WTs in distribution network. Stochastic nature of solar and wind power generation was considered in the paper to minimize active energy loss. Alsayed et al. [9] have investigated combined PV–WT sizing problem with multi criteria decision making algorithm (MCDA). Environmental and economical attributes are weighted based on their entropy variation due to change of generation and load. Later in Ref. [10], they have exploited non-dominated sorting genetic algorithm (NSGA) along with MCDA for optimum design of the hybrid system configuration.

Capacitor placement problems for distribution network were discussed in Refs. [11–13]. The optimal locations and sizes of capacitor banks were obtained using a direct search algorithm in Ref. [11]. The aim of the study was to minimize the cost related to capacitor planning. A bacterial foraging based solution methodology was proposed in Ref. [12] to find the optimal location and size of capacitors in radial distribution systems. A teaching learning based optimization algorithm was presented in Ref. [13] to minimize active network power loss, capacitor installation cost and energy loss cost. However, there is hardly any paper addressing the issues regarding combined planning of PV array, WT and capacitor bank.

Few recent researches have examined distribution planning problem incorporating local generation and capacitor unit [14–16]. An analytical based approach for allocation of distributed generation (DG) and capacitor was presented by Naik et al. [14] on view point of minimization of total real power loss. Sensitivity analysis has been performed to identify the candidate locations for DG and capacitor placement, and the heuristic curve fitting technique used to determine their capacity. In Ref. [15], authors have proposed simultaneous placement of DG and capacitor in radial distribution system considering the objectives of energy loss minimization and voltage profile improvement. A combinatorial form of local search and genetic algorithm was utilized to solve the optimization problem. Moradi et al. [16] presented imperialist competitive algorithm approach to identify location and capacity of DG and capacitor in distribution network for power loss reduction and voltage stability improvement. In these studies DGs were considered as constant power sources (constant PQ model). However, integration of intermittent RESs cannot guarantee constant power output throughout the planning period. Therefore, it is important to assess and quantify the relative system performance with the integration of RES units whose generation varies daily or seasonally.

This paper presents a novel multi objective particle swarm optimization (MOPSO) technique based planning method for appropriate location and size selection of non-dispatchable RESs and capacitor banks in an existing operation situation. Load growth is a continual phenomenon of distribution network which is unavoidable. The network operational characteristics would likely to be affected by the additional demand. In previous studies the effect of load growth was not considered. In this paper, a proper approach for a well-planned distribution system is convinced while considering the impact of yearly load growth. The rest of this paper is organized as follows. In Section 'Modelling of intermittent RESs', probabilistic power generation model of RESs considering stochastic nature of resources has been presented. Section 'Planning problem' illustrates the proposed planning problem with formulation of objective functions and constraints as well. In Section 'Application of MOPSO', MOPSO technique based solution strategy to design sustainable distribution network is discussed. Section 'Test network and local weather' contains description of test network and details about the weather affecting the distribution system. Simulation results are discussed in Section 'Results and discussion' and finally the conclusions are reported in Section 'Conclusion'.

Modelling of intermittent RESs

Solar and wind power generations are highly influenced by meteorological conditions such as wind speed, solar irradiance, and ambient temperature. So the characteristics of solar radiation and wind conditions at installation location should be analyzed at the primary stage for efficient utilization of PV arrays and WTs.

Renewable resource model

Probability distribution functions (PDF) can be used to characterize stochastic behavior of renewable resources (wind speed and solar irradiance) in a statistical manner.

Solar irradiance modelling

The probabilistic nature of solar irradiance is considered to follow Beta PDF [17,18]. Beta distribution for solar irradiance s^t (kW/m^2) over time segment 't' is given by

$$f_s^t(s) = \frac{\Gamma(\alpha^t + \beta^t)}{\Gamma(\alpha^t)\cdot\Gamma(\beta^t)} \cdot (s^t)^{\alpha^t - 1} \cdot (1 - s^t)^{\beta^t - 1} \quad \text{for} \quad \alpha^t > 0; \quad \beta^t > 0 \tag{1}$$

where α^t and β^t are the shape parameters at 't'; and Γ represents Gamma function.

Shape parameters of Beta PDF can be calculated using mean (μ_s^t) and standard deviation (σ_s^t) of irradiance for corresponding time segment.

$$\beta^t = (1 - \mu_s^t) \cdot \left(\frac{\mu_s^t (1 + \mu_s^t)}{(\sigma_s^t)^2} - 1 \right) \tag{2}$$

$$\alpha^t = \frac{\mu_s^t * \beta^t}{(1 - \mu_s^t)} \tag{3}$$

Wind speed modelling

In order to describe stochastic behavior of wind speed in a predefined time period, Weibull PDF has been chosen [8,18]. Weibull distribution for the wind speed v^t (m/s) at tth time segment can be expressed as

$$f_v^t(v) = \frac{k^t}{c^t} \cdot \left(\frac{v^t}{c^t} \right)^{k^t - 1} \cdot \exp\left(- \left(\frac{v^t}{c^t} \right)^{k^t - 1} \right) \quad \text{for} \quad c^t > 1; \quad k^t > 0 \tag{4}$$

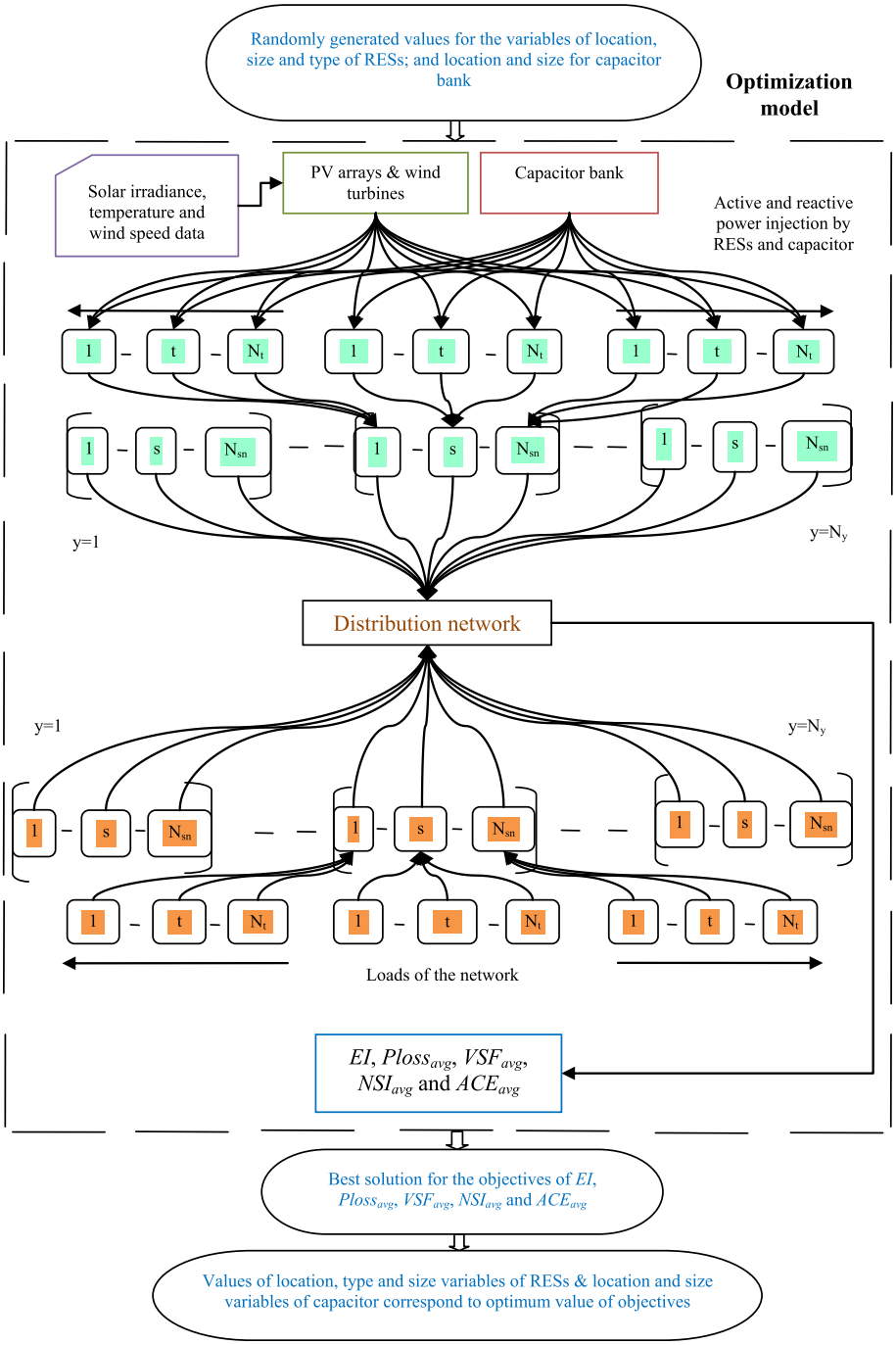

Fig. 1. Optimization framework considering time varying generation and load.

The shape parameters k^t and c^t are calculated as follows.

$$k^t = \left(\frac{\sigma^t}{\mu_v^t}\right)^{-1.086} \tag{5}$$

$$c^t = \frac{\mu_v^t}{\Gamma(1+1/k^t)} \tag{6}$$

μ_v^t and σ_v^t are mean and standard deviation of wind speed at time segment 't'.

Power generation model

To calculate the output power of intermittent RESs, the continuous PDF for a specific time segment has been divided into states (periods), in each of which the solar irradiance and wind speed are within specific limits [17]. Power generation of PV array and WT are governed by probability of all possible states in the time segment.

Power generation by PV array

The average output power of PV array correspond to a specific time segment 't' (P_{PV}^t) can be calculated as follows.

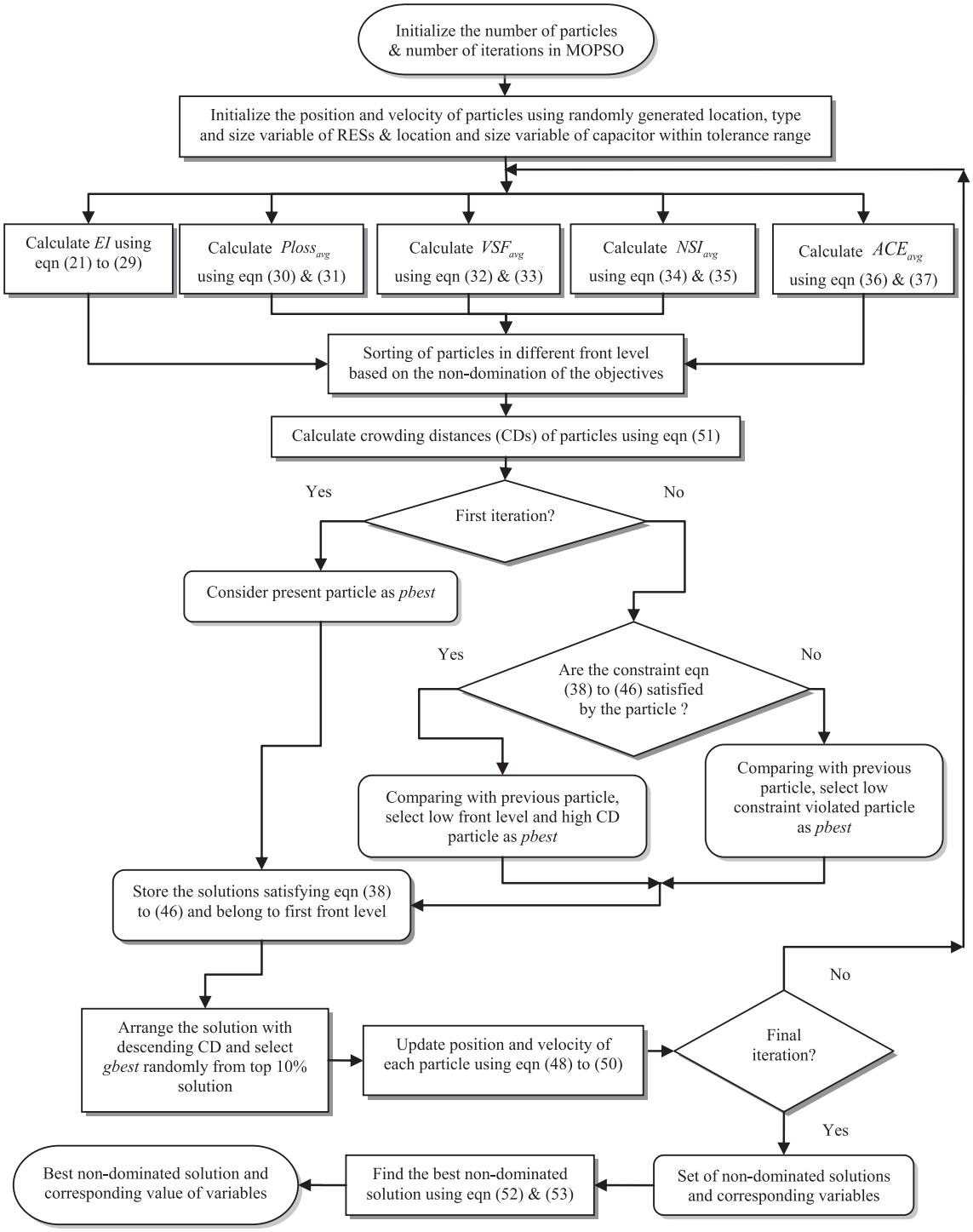

Fig. 2. Flowchart to generate best non-dominated solution from multi-objective RES–capacitor planning problem.

$$P_{PV}^{t} = \sum_{g=1}^{N_s} PG_{PVg} * P_s\left(s_g^t\right) \tag{7}$$

where 'g' signifies the state variable and N_s is the number of discrete solar irradiance state. s_g^t is the gth level/state of solar irradiance at tth time segment.

The probability of the solar irradiance for each state during any specific time frame is calculated as

$$P_s\left(s_g^t\right) = \begin{cases} \int_0^{(s_g^t + s_{g+1}^t)/2} f_s^t(s)ds & \text{for} \quad g = 1 \\ \int_{(s_{g-1}^t + s_g^t)/2}^{(s_g^t + s_{g+1}^t)/2} f_s^t(s)ds & \text{for} \quad g = 2 \ldots (N_s - 1) \\ \int_{(s_{g-1}^t + s_g^t)/2}^{\infty} f_s^t(s)ds & \text{for} \quad g = N_s \end{cases} \tag{8}$$

Solar irradiance and ambient temperature of the site are the main dominating factors which affect the output power of PV array. The power generation of PV array at average solar irradiance (s_{ag}) for the gth level/state is evaluated as

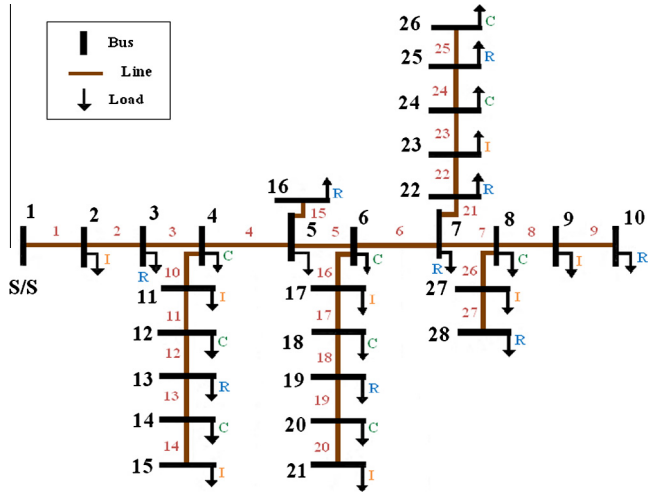

Fig. 3. Single line diagram of test distribution network (S/S: substation; R: residential demand; C: commercial demand and I: industrial demand).

$$PG_{PVg}(s_{ag}) = N_{PV\mathrm{mod}} * FF * V_g * I_g \tag{9}$$

where $N_{PV\mathrm{mod}}$ is the total number of PV modules used to form a PV array. The current–voltage characteristic of a PV module can be determined for a given radiation level and ambient temperature T_A (°C) using the following relations [19].

$$I_g = s_{ag}[I_{SC} + K_i(T_C - 25)] \tag{10}$$

$$V_g = V_{OC} - K_v * T_{cg} \tag{11}$$

$$T_{cg} = T_A + s_{ag}\left(\frac{N_{OT} - 20}{0.8}\right) \tag{12}$$

$$FF = \frac{V_{MPP} * I_{MPP}}{V_{OC} * I_{SC}} \tag{13}$$

Table 2
Exponent of voltage for active and reactive power in different class of loads.

Load type	Exponent for active power	Exponent for reactive power
Residential	0.92	4.04
Commercial	1.51	3.40
Industrial	0.18	6.0

T_{cg} is cell temperature at gth state (°C); K_i and K_v are current and voltage temperature co-efficient (A/°C and V/°C); N_{OT} is the nominal operating temperature of cell (°C); FF is the fill factor; V_{OC} and I_{SC} are open circuit voltage (V) and short circuit current (A); V_{MPP} and I_{MPP} are respectively voltage (V) and current (A) at maximum power point;

Power generation by wind turbine

The average output power of WT corresponds to a specific tth time segment (P^t_{WT}) can be calculated as follows.

$$P^t_{WT} = \sum_{g=1}^{N_v} PG_{WTg} * P_v\left(v^t_g\right) \tag{14}$$

The probability of the wind speed for each state during any specific time frame is calculated as

$$P_v\left(v^t_g\right) = \begin{cases} \int_0^{(v^t_g + v^t_{g+1})/2} f^t_v(v)dv & \text{for} \quad g = 1 \\ \int_{(v^t_{g-1} + v^t_g)/2}^{(v^t_g + v^t_{g+1})/2} f^t_v(v)dv & \text{for} \quad g = 2 \ldots (N_v - 1) \\ \int_{(v^t_{g-1} + v^t_g)/2}^{\infty} f^t_v(v)dv & \text{for} \quad g = N_v \end{cases} \tag{15}$$

Power generation of WT depends on its power performance curve. For non-liner performance characteristics, power generation of WT [18] at average wind speed (v_{ag}) for state 'g' is calculated as

$$PG_{WTg} = \begin{cases} 0 & v_{ag} < v_{cin} \quad \text{or} \quad v_{ag} > v_{cout} \\ (a * v^3_{ag} + b * P_{rated}) & v_{cin} \leqslant v_{ag} \leqslant v_N \\ P_{rated} & v_N \leqslant v_{ag} \leqslant v_{cout} \end{cases} \tag{16}$$

Table 1
Line and load data of 28-bus distribution network.

Line number	Sending End (SE) bus	Receiving End (RE) bus	Resistance of line section SE–RE (ohm)	Reactance of line section SE–RE (ohm)	Maximum line loading (MVA)	Peak load at RE bus (MVA)
1	1	2	1.179	0.82	1.5	0.050
2	2	3	1.796	1.231	1.3	0.020
3	3	4	1.306	0.895	1.1	0.050
4	4	5	1.851	1.266	0.8	0.020
5	5	6	1.524	1.044	0.7	0.050
6	6	7	1.905	1.305	0.6	0.050
7	7	8	1.197	0.820	0.5	0.050
8	8	9	0.653	0.447	0.4	0.020
9	9	10	1.143	0.783	0.3	0.020
10	4	11	2.823	1.172	0.5	0.080
11	11	12	1.184	0.491	0.4	0.050
12	12	13	1.002	0.416	0.3	0.050
13	13	14	0.455	0.189	0.2	0.020
14	14	15	0.546	0.227	0.1	0.050
15	5	16	2.550	1.058	0.1	0.050
16	6	17	1.366	0.567	0.5	0.013
17	17	18	0.819	0.340	0.4	0.013
18	18	19	1.548	0.642	0.3	0.050
19	19	20	1.366	0.567	0.2	0.050
20	20	21	3.522	0.340	0.1	0.020
21	7	22	1.548	0.642	0.5	0.050
22	22	23	1.092	0.453	0.4	0.013
23	23	24	0.910	0.378	0.3	0.080
24	24	25	0.455	0.189	0.2	0.013
25	25	26	0.364	0.151	0.1	0.050
26	8	27	0.546	0.226	0.2	0.050
27	27	28	0.273	0.113	0.1	0.050

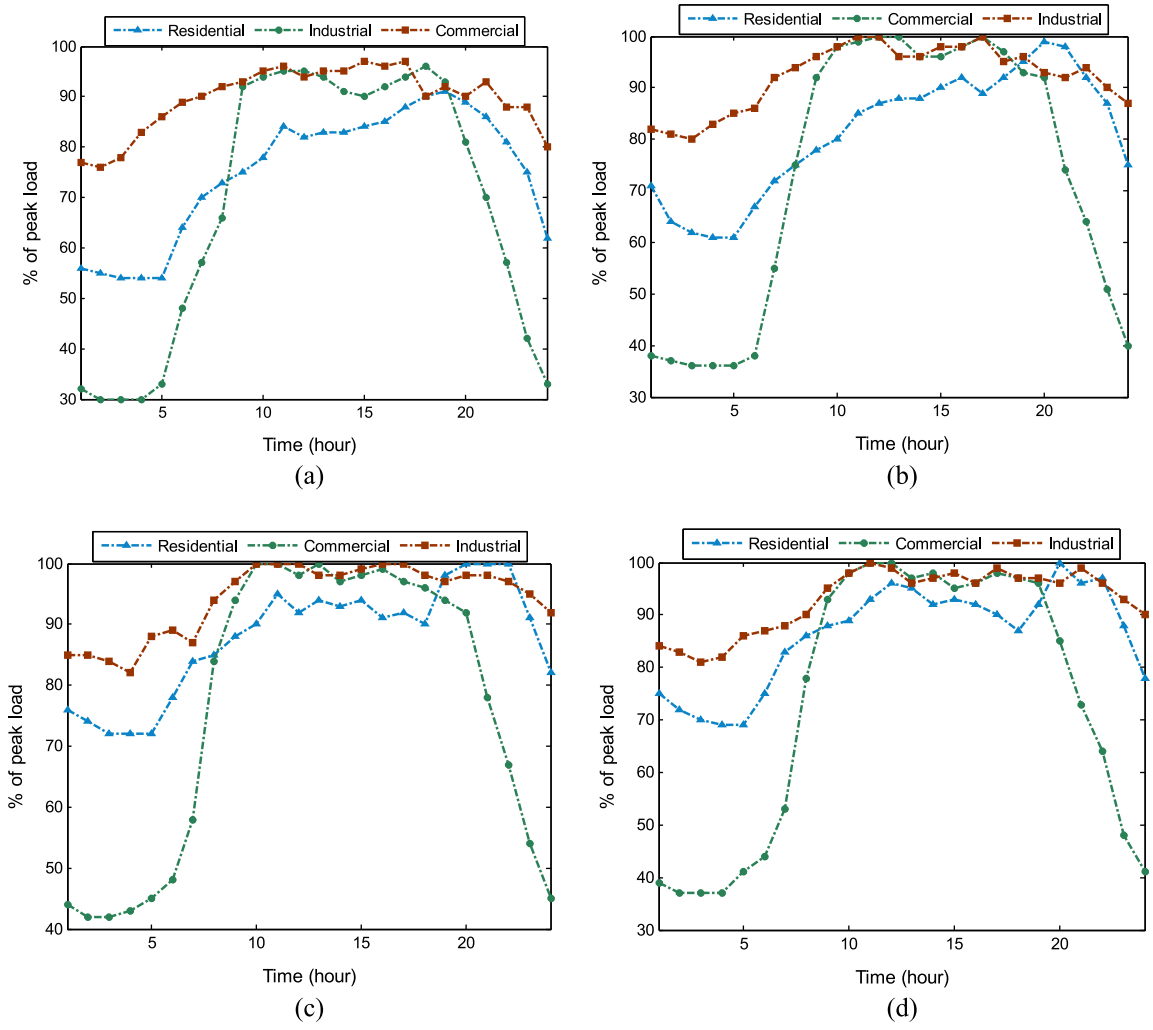

Fig. 4. Variation of load demand for residential, commercial and industrial customers during. (a) Winter. (b) Spring. (c) Summer. (d) Autumn.

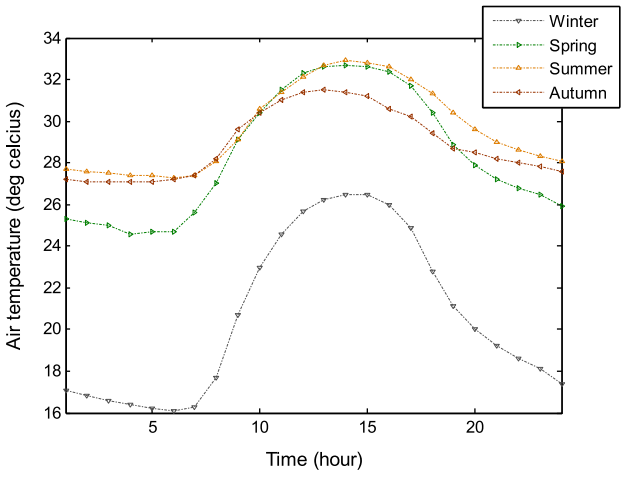

Fig. 5. Variation of ambient temperature in different seasons at test site.

where P_{rated} is the maximum power that can be generated by WT; v_{cout} is the cut-out wind speed; Constants a and b are function of cut-in wind speed (v_{cin}) and nominal wind speed (v_N), and obtained as

$$a = \frac{P_{rated}}{(v_N^3 - v_{cin}^3)} \tag{17}$$

$$b = \frac{v_{cin}^3}{(v_N^3 - v_{cin}^3)} \tag{18}$$

Planning problem

Concurrent allocation of RESs and capacitor banks in distribution network is a nonlinear multitask optimization problem, including some equality and inequality constraints. Multitask includes maximization of economic benefit from the project, minimization of network power loss, enhancement of voltage stability, augmentation of network security and mitigation of carbon emission satisfying voltage limit, line capacity, RES penetration and capacitor penetration constraints. RESs are considered to be operated at unity power factor because cost of real power is higher compared to reactive power. The effect of load growth has been taken into account to model the planning problem.

Load growth

The effect of the load growth results a considerable increment in customer demand after a certain time interval. The modified

Table 3
Mean and standard deviation of solar irradiance (kW/m^2) in the study period.

Hour	Winter		Spring		Summer		Autumn	
	μ_s	σ_s	μ_s	σ_s	μ_s	σ_s	μ_s	σ_s
1	0	0	0	0	0	0	0	0
2	0	0	0	0	0	0	0	0
3	0	0	0	0	0	0	0	0
4	0	0	0	0	0	0	0	0
5	0	0	0	0	0.0032	0.0045	0	0
6	0.0300	0.0417	0.0158	0.0196	0.1278	0.0406	0.0707	0.0299
7	0.1623	0.0463	0.1605	0.0332	0.2538	0.0714	0.2177	0.0433
8	0.3741	0.0669	0.3412	0.0658	0.3824	0.1189	0.3988	0.0803
9	0.4732	0.0669	0.5060	0.1002	0.4908	0.1388	0.5465	0.1121
10	0.5831	0.0998	0.6385	0.1319	0.5680	0.1659	0.6442	0.1336
11	0.6463	0.1219	0.7120	0.1551	0.6164	0.1445	0.6827	0.1492
12	0.6496	0.1262	0.7305	0.1510	0.5990	0.1175	0.6645	0.1452
13	0.5921	0.1117	0.6780	0.1283	0.5614	0.0995	0.5923	0.1282
14	0.4786	0.0838	0.5699	0.1011	0.4672	0.0788	0.4731	0.0999
15	0.3228	0.0515	0.4124	0.0765	0.3548	0.0550	0.3121	0.0635
16	0.1609	0.0382	0.2394	0.0446	0.2228	0.0410	0.1402	0.0309
17	0.0269	0.0372	0.0834	0.0230	0.1030	0.0276	0.0057	0.0112
18	0	0	0	0	0	0	0	0
19	0	0	0	0	0	0	0	0
20	0	0	0	0	0	0	0	0
21	0	0	0	0	0	0	0	0
22	0	0	0	0	0	0	0	0
23	0	0	0	0	0	0	0	0
24	0	0	0	0	0	0	0	0

Table 4
Mean and standard deviation of wind speed (m/s) in the study period.

Hour	Winter		Spring		Summer		Autumn	
	μ_v	σ_v	μ_v	σ_v	μ_v	σ_v	μ_v	σ_v
1	2.1333	1.1676	10.7000	3.0643	9.9000	0.7937	3.9667	2.5146
2	2.2333	1.0693	10.5667	2.7647	9.3667	0.8021	3.8667	2.2301
3	2.5000	1.0000	10.3667	2.9501	9.1667	0.8505	3.8333	2.0648
4	2.7333	0.8021	9.9333	3.1005	9.0000	0.8185	3.8000	2.0075
5	2.9333	0.8021	9.6000	3.0512	8.7000	0.7550	3.7667	1.8717
6	2.9667	0.6807	9.6667	3.0892	8.6000	1.0583	3.9000	1.7776
7	3.0667	0.6506	9.6333	3.2347	9.0000	1.1533	4.3333	2.0526
8	3.8333	0.7095	10.0333	2.9143	9.0333	1.1504	5.0000	1.7059
9	5.1000	0.8185	10.1667	2.4826	9.3333	0.9504	5.5667	1.6073
10	5.5667	0.6110	10.5333	2.3459	9.6000	1.1533	5.8667	1.2423
11	5.9333	0.3055	11.0000	2.5515	10.1333	1.0066	6.2333	1.6166
12	6.1000	0.3606	11.2333	2.5891	10.2667	0.8622	6.1667	1.5144
13	3.9333	0.3215	6.2667	0.6807	7.9667	0.3786	5.3000	0.8718
14	3.8000	0.5292	6.3333	0.7506	8.0000	0.4583	5.2333	1.0116
15	3.6000	0.5292	5.6000	0.3606	8.0000	0.5000	4.8667	1.0693
16	3.0000	0.5568	5.8333	0.6506	7.7333	0.4509	4.3000	1.1358
17	2.0667	0.9609	5.3667	1.2014	6.9667	0.2309	3.3000	1.5395
18	0.8333	0.5132	4.0667	1.7559	5.9667	0.3786	1.9333	1.2858
19	0.6333	0.2517	2.8667	1.3013	4.8333	0.3215	1.5667	1.0786
20	0.7000	0.3000	2.7333	1.0017	4.4333	0.3215	1.5000	0.8718
21	0.8667	0.4509	2.8000	0.8888	4.3333	0.4163	1.5667	0.9074
22	0.9333	0.4041	2.8000	0.7937	4.1000	0.2646	1.5000	0.9644
23	0.9000	0.3606	2.8333	0.6351	4.0667	0.2082	1.5333	0.9292
24	0.9667	0.3215	2.9000	0.6083	4.0000	0.1732	1.5333	0.8386

Table 5
Specification of PV module.

Parameter	Value
Voltage at maximum power point	28.36 V
Voltage at maximum power point	7.76 A
Open circuit voltage	36.96 V
Short circuit current	8.38 A
Nominal cell operating temperature	43 °C
Current temperature co-efficient	0.00545 A/°C
Voltage temperature co-efficient	0.1278 V/°C
Life period	20 years

Table 6
Technical specification of wind turbine.

Attribute	Value
Cut-in-speed	3 m/s
Nominal wind speed	12 m/s
Cut-out speed	25 m/s
Rated output power	250 kW
Life period	20 years

Table 7
Cost attributes of RESs (55INR = 1$).

	Investment cost (INR/kW)	Operating & maintenance cost (INR/kW)
Solar power generation unit	71,250	1425 (2% of Investment)
Wind power generation unit	67,890	3395 (5% of Investment)

Table 8
Technical and economic specification of capacitor bank.

Attribute	Value
Rated output	150 kVAR
Cost	41,250 INR
Life period	10 years

Table 9
Value of the objective functions for different non-dominated solutions.

Non-dominated solution	$-EI$	$Ploss_{avg}$	$-VSF_{avg}$	NSI_{avg}	ACE_{avg}
1	−1.8145	0.0223	−0.9610	0.3543	4182
2	−1.8013	0.0242	−0.9620	0.4049	4379
3	−1.6353	0.0386	−0.9455	0.3763	4777
4	−2.8168	0.0296	−0.9551	0.3755	5534
5	−2.1866	0.0270	−0.9562	0.3766	5160
6	−1.8588	0.0267	−0.9583	0.3864	4417
7	−1.7927	0.0260	−0.9589	0.3709	4919
8	−1.9691	0.0280	−0.9545	0.3557	4622
9	−1.7086	0.0335	−0.9498	0.3705	4576
10	−1.7829	0.0267	−0.9572	0.3596	4916
11	−1.8070	0.0241	−0.9603	0.3589	4551
12	−1.9860	0.0295	−0.9524	0.3583	4804
13	−1.9768	0.0300	−0.9520	0.3728	4804

active and reactive annual peak electric load (APEL) for x% of annual load growth at bus-i for yth year becomes

$$P_{D,i}^{y} = \left(1 + \frac{x}{100}\right)^{y} P_{D,i} \tag{19}$$

$$Q_{D,i}^{y} = \left(1 + \frac{x}{100}\right)^{y} Q_{D,i} \tag{20}$$

$P_{D,i}$ and $Q_{D,i}$ are active and reactive power demand of bus-i at the initial stage of planning.

Objective functions

EI, VSF, NSI and ACE are utilized to quantify economic benefit, voltage stability condition of the network, power congestion risk of the network and carbon oxide emission due to grid power consumption in the network respectively. It is noteworthy to be mentioned that voltage magnitude of the buses and the line power flows change from year to year due to load growth. Complying with the fact, EI is calculated considering reduction of power losses for distinct years. Also average value of active power loss ($Ploss_{avg}$), VSF (VSF_{avg}), NSI (NSI_{avg}) and ACE (ACE_{avg}) over the planning horizon are suggested as objective functions.

Table 11
Measurement of economical, technical and environmental parameters before and after application of RESs and capacitor bank.

	Value of EI	$Ploss_{avg}$ (MW)	Value of VSF_{avg}	Value of NSI_{avg}	ACE_{avg} (ton/year)
Network without RESs & capacitor bank	–	0.0439	0.9406	0.3853	5760
Network with RESs & capacitor bank	1.8145	0.0223	0.9610	0.3543	4182

Economic index

An EI is formulated to measure the economical potential of the project over the planning period. Different financial aspects related to reinforcement of RESs and capacitor banks are needed to be investigated to develop EI.

Annualized capital cost of RESs. Annual capital cost [20] for RESs can be represented as

$$ACP_{RES} = \sum_{i=2}^{N_b} \sum_{j \in type} (IC_{RES,ij} * n_i * l_i) * CRF(IR, LP_j) \tag{21}$$

Investment cost of RES includes purchase, transportation and connection cost of PV arrays and WTs. $IC_{RES,ij}$ is the initial investment for type-j RES unit at bus-i. LP_j is the life period of type-j RES. N_b is the total number of buses present in the distribution network. l_i and n_i are the location and size variable for RES at bus-i respectively. It is to be noted that value of l_i equals to 0 and 1 signifies connection and disconnection of DG at bus-i. CRF is the capital recovery factor which signifies the present value of an annuity (a series of equal annual cash flows). CRF depends on annual real interest rate and life period of the component. CRF can be obtained as follows

$$CRF = \frac{IR \cdot (1 + IR)^{LP}}{(1 + IR)^{LP} - 1} \tag{22}$$

The annual real interest rate IR is related to the nominal interest rate (IR') and inflation rate (IF) by the following equation

$$IR = \frac{(IR' - IF)}{(1 + IF)} \tag{23}$$

Annualized capital cost of capacitor banks. The annualized capital cost of capacitor banks is given by

$$ACP_{cap} = \sum_{i=2}^{N_b} (IC_{Cap,i} * m_i * c_i) * CRF \tag{24}$$

where IC_{cap} is the initial investment for the capacitor banks; c_i and m_i are the location and size variable for capacitor bank at bus-i respectively.

Table 10
Optimum location and size of PV arrays, WTs and capacitor banks in distribution network.

Intermittent RESs				Capacitor banks		
Location in network	Type of generation	Number of installed unit	Total size at location	Location	Number of installed unit	Total size at location
Bus-7	Solar	2	264 kW	Bus-6	2	300 kVAR
Bus-13	Wind	2	500 kW			
Bus-17	Solar	2	264 kW			

Table 12
Comparative study of economical, technical and environmental prospects at different system configuration.

	Value of *EI*	$Ploss_{avg}$ (MW)	Value of VSF_{avg}	Value of NSI_{avg}	ACE_{avg} (ton/year)
Network with intermittent RESs only	1.7809	0.0346	0.9508	0.3694	4267
Network with capacitor bank only	82.0311	0.0304	0.9536	0.3650	5712
Network with intermittent RESs & capacitor bank	1.8145	0.0223	0.9610	0.3543	4182

Annualized operating and maintenance cost of RESs. Operating and maintenance cost includes yearly labor cost for service, tax and maintenance cost of PV array and WTs. Annualized operating and maintenance cost of RESs can be represented as

$$AOMC_{RES} = \frac{\sum_{y=1}^{N_y}\left(\sum_{i=2}^{N_b}\sum_{j\in type} OMC_{RES,ij} * n_i * l_i\right) * CPV^y}{N_y} \quad (25)$$

$OMC_{RES,ij}$ is the operating and maintenance cost per year for type-*j* RES technology at bus-*i*. N_y is the planning period in years. CPV converts the future cost into its equivalent present value and can be realized as

$$CPV^y = \left(\frac{1+IF}{1+IR'}\right)^y \quad (26)$$

Annualized purchased power cost saving. Deployment of RESs and capacitor banks in distribution network drastically reduce grid power consumption because of DISCO's localized generation and network power loss reduction. Hence considerable amount of energy cost is saved by DISCO.

Annual cost saving due to reduction of purchased power can be determined as

$$ACS = \frac{\sum_{y=1}^{N_y}\left(\Delta Ploss^y + \sum_{i=1}^{N_b} P^y_{RES,i} * n_i * l_i\right) * CPV^y * C_{hr}}{N_y} \quad (27)$$

$P^y_{RES,i}$ is the total active power injection by RES unit at bus-*i* in *y*th year. $\Delta Ploss^y$ is the reduction of network real power loss in the year

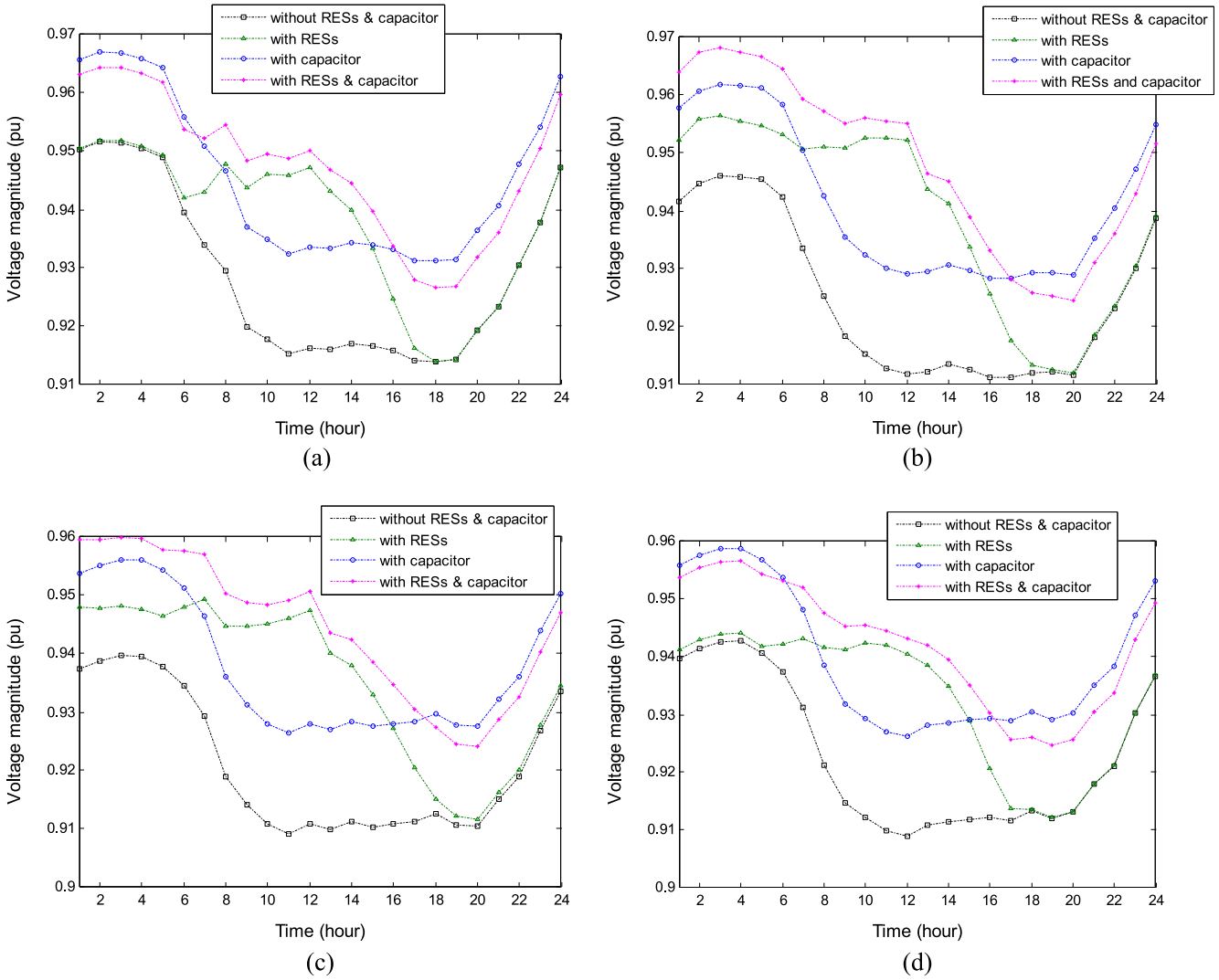

Fig. 6. Illustration of system's minimum bus voltage at different penetration scenario during. (a) Winter. (b) Spring. (c) Summer. (d) Autumn.

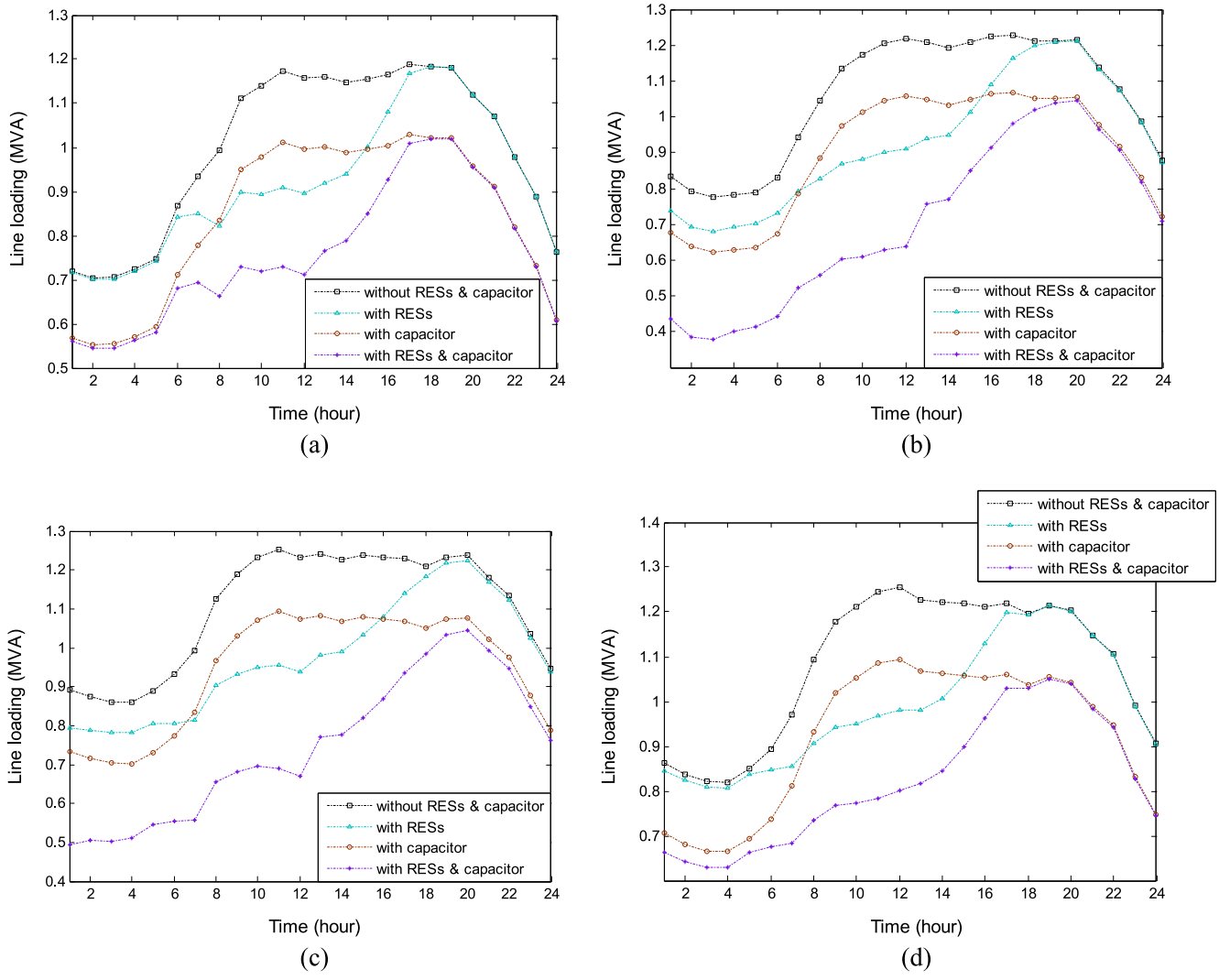

Fig. 7. Illustration of maximum line loading for RES penetration, capacitor penetration and RES–capacitor penetration during. (a) Winter. (b) Spring. (c) Summer. (d) Autumn.

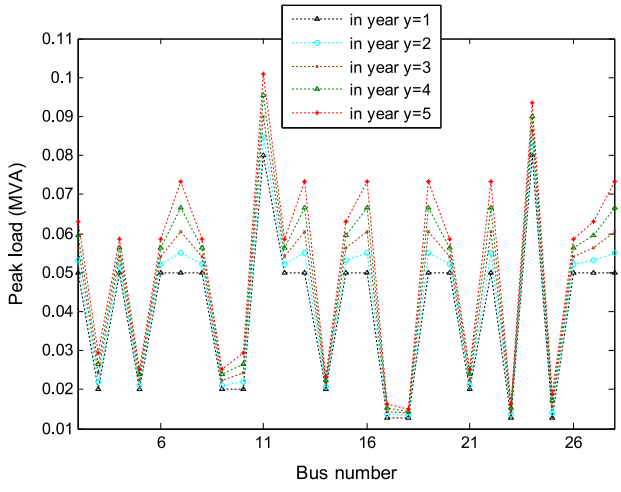

Fig. 8. Variation of APEL at the load buses in the different years of the study period.

'y' due to reinforcement. C_{hr} is the cost of grid power. P^{y}_{RES} can be calculated using the following equation.

$$P^{y}_{RES} = \left\{ \sum_{sn=1}^{N_{sn}} \sum_{t=1}^{N_t} \sum_{j \in type} \left(P^{t}_{RES,j} \right)^{sn} \right\} * \left(\frac{24}{N_t} \right) * \left(\frac{N_{Dy}}{N_{sn}} \right) \tag{28}$$

$P^{t}_{RES,j}$ would be P^{t}_{PV} and P^{t}_{WT} for the case of solar and wind power generation respectively. N_t and N_{sn} are the total number time segment in a season and total number of season in a year respectively. N_{Dy} is the number of days in a year in which RESs are available for power generation.

Considering the annual cash inflow and outflow of combined RES–capacitor planning project, EI is formulated as

$$EI = \frac{ACS}{(ACP_{RES} + ACP_{cap} + AOMC_{RES})} \tag{29}$$

The higher value of EI indicates elevated profit margin for the utilities.

Average active power loss

Penetration of RESs and capacitor banks creates significant impact on real power losses of the distribution network. Average real power loss in presence of RESs and capacitors is obtained as

$$Ploss_{avg} = \frac{\sum_{y=1}^{N_y} \sum_{sn=1}^{N_{sn}} \sum_{t=1}^{N_t} \left((Ploss^{t})^{sn} \right)^{y}}{(N_y * N_{sn} * N_t)} \tag{30}$$

Table 13
Network performance parameters in presence and absence of load growth.

	$Ploss_{avg}$ (MW)	Value of VSF_{avg}	Value of NSI_{avg}
Without load growth	0.0338	0.9478	0.3419
With load growth	0.0439	0.9406	0.3853

$Ploss^t$ is the real power loss of total distribution network at tth} hour which can calculated using the following equation

$$Ploss^t = \sum_{i=1}^{N_{br}} \sum_{j \in type} \frac{\left\{ \left(P^t_{D,i+1} - P^t_{RES,i+1,j} * n_i * l_i \right)^2 + \left(Q^t_{D,i+1} - Q^t_{cap,i+1} * m_i * c_i \right)^2 \right\}}{\left(V^t_{i+1} \right)^2} . r_i \tag{31}$$

$Q^t_{cap,i+1}$ is the reactive power supplied by capacitor banks at bus-i + 1 in 't' time frame. N_{br} is the total number of branches or lines present in the network and r_i is the resistance of line-i.

Average voltage stability factor

Voltage stability indices [21–23] are widely used tool to measure the proximity of buses towards voltage collapse point. A voltage stability index namely VSF [24] is reproduced here to quantify the voltage stability condition of total distribution network. VSF for time segment 't' can be represented as

$$VSF^t = \frac{\sum_{i=2}^{N_b} (2V^t_i - V^t_{i-1})}{(N_b - 1)} \tag{32}$$

Average voltage stability level for the planning period can be formulated as

$$VSF_{avg} = \frac{\sum_{y=1}^{N_y} \sum_{sn=1}^{N_{sn}} \sum_{t=1}^{N_t} \left((VSF^t)^{sn} \right)^y}{(N_y * N_{sn} * N_t)} \tag{33}$$

According to the authors' investigation higher value of VSF_{avg} indicates more stable voltage stability condition of the network.

Average network security index

NSI is an indicator to measure the level of risk for power flow in the network before going to extremis [25,26]. NSI at tth time segment can be formulated as

$$NSI^t = \frac{\sum_{i=1}^{N_{br}} \frac{L^t_{MVA_i}}{L_{MVAmax,i}}}{N_{br}} \tag{34}$$

$L^t_{MVA,i}$ is the power flow (MVA) through line-i at tth time segment and $L_{MVAmax,i}$ is the maximum capacity of power flow for line-i.

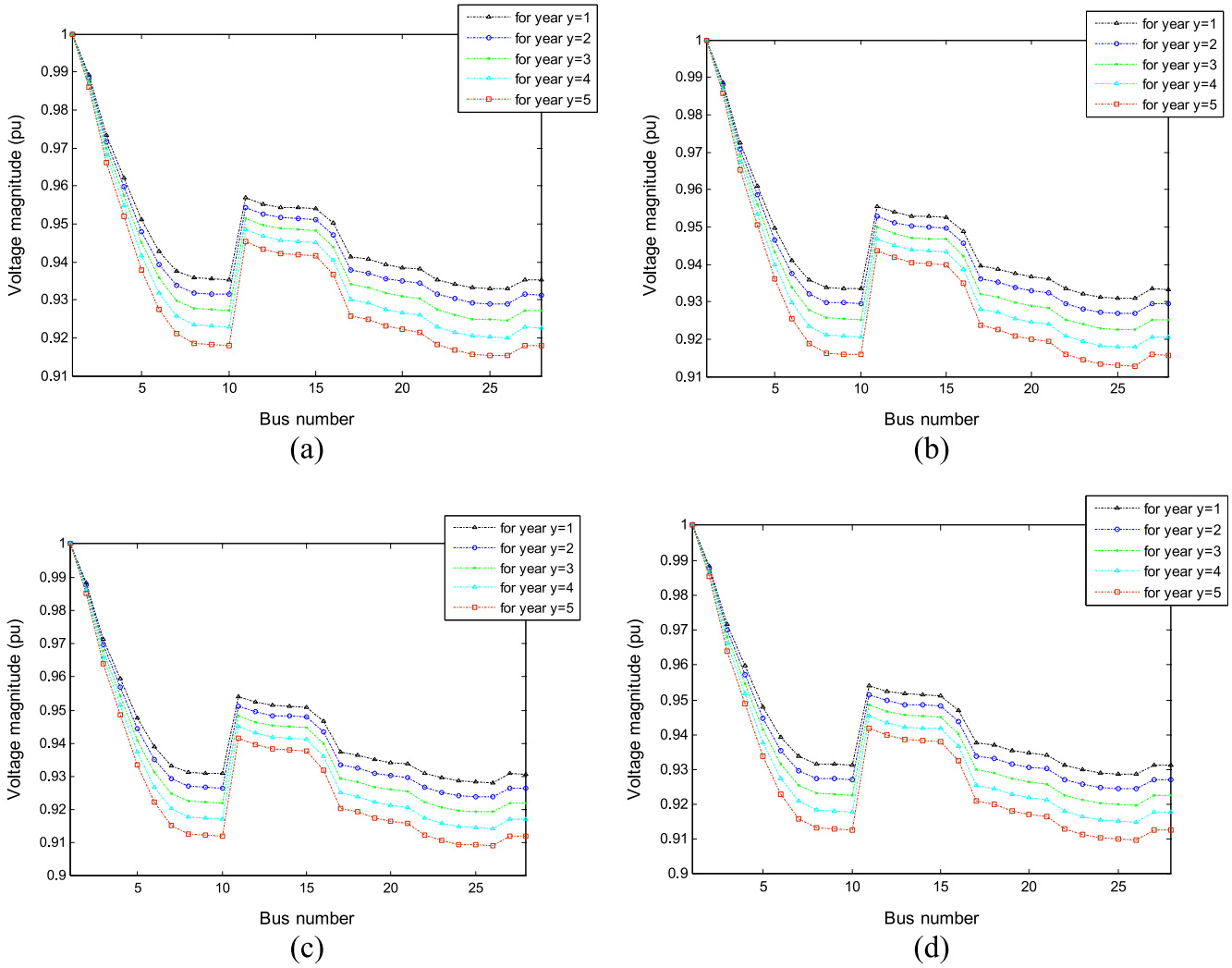

Fig. 9. Impact of load growth on voltage magnitude at buses during time period 10.00–11.00 h in (a) Winter. (b) Spring. (c) Summer. (d) Autumn.

Average value of NSI in the planning horizon is realized as

$$NSI_{avg} = \frac{\sum_{y=1}^{N_y}\sum_{sn=1}^{N_{sn}}\sum_{t=1}^{N_t}\left((NSI^t)^{sn}\right)^y}{(N_y * N_{sn} * N_t)} \tag{35}$$

The decreased value of *NSI* refers to an improvement in security margin for the whole distribution network.

Average annual carbon-di-oxide emission

Transmission grid power which is mainly coming from thermal power plants is responsible for abundant emission of carbon-di-oxide. IEA have predicted that excessive carbon-di-oxide emissions into the atmosphere will increase the earth's surface temperature approximately 3.6 °C by the next 25 years [27]. Accumulation of carbon-di-oxide in the atmosphere creates detrimental effect on global climate change by warming the earth surface. This effect is associated with the absorption of long wavelength radiation much more by carbon-di-oxide than other gases. Worldwide urge to mitigate greenhouse gas emissions has increased pressure to alter current generation and distribution paradigm. This is leading to a new era in which renewable power generation technologies are growing against the backdrop of existing power delivery system.

The total annual carbon-di-oxide emission from hybrid power system can be expressed as

$$ACE_{avg} = \frac{\sum_{y=1}^{N_y}\sum_{sn=1}^{N_{sn}}\sum_{t=1}^{N_t}\left((PG_{SS}^t)^{sn}\right)^y * \left(\frac{24}{N_t}\right) * \left(\frac{365}{N_{sn}}\right) * ER_c}{N_y} \tag{36}$$

PG_{SS}^t is the active grid power consumption through substation at tth time segment and ER_c is the carbon-di-oxide emission rate. PG_{SS}^t can be obtained from the equation given below

$$PG_{SS}^t = \sum_{i=2}^{N_b} P_{D,i}^t + Ploss^t - \sum_{i=2}^{N_b}\sum_{j\in type} P_{RES,ij}^t * n_i * l_i \tag{37}$$

Operational constraints

The planning problem is formulated to meet multiple objective functions satisfying the equality and inequality constraints as given below

Power flow constraint:

$$PG_{SS}^t + \sum_{i=2}^{N_b}\sum_{j\in type} P_{RES,ij}^t * n_i * l_i - \sum_{i=2}^{N_b} P_{D,i}^t - Ploss^t = 0 \tag{38}$$

$$QG_{SS}^t + \sum_{i=2}^{N_b} Q_{cap,i}^t * m_i * c_i - \sum_{i=2}^{N_b} Q_{D,i}^t - Qloss^t = 0 \tag{39}$$

QG_{SS}^t is the reactive power consumption through substation at tth time segment. $Qloss^t$ is reactive power loss of network at tth time segment.

RES penetration constraint at bus-i:

$$P_{RES}^t * n_i \leqslant P_{RES}^t * n_{\max,i} \tag{40}$$

$n_{\max,i}$ is the maximum number of RES unit that can be accommodated at bus-i.

Capacitor penetration constraint at bus-i:

$$Q_{cap}^t * m_i \leqslant Q_{cap}^t * m_{\max,i} \tag{41}$$

$m_{\max,i}$ is the maximum number of capacitor bank that can be connected to bus-i.*Bus voltage constraint at bus-i*:

$$V_i^t \leqslant V_{\max,i} \tag{42}$$

V_i^t and $V_{\max,i}$ are actual and maximum voltage magnitude of bus-i at tth time segment.

Line capacity constraint of line-i:

$$L_{MVA,i}^t \leqslant L_{MVA\max,i} \tag{43}$$

RES penetration constraint in network:

$$\sum_{i=2}^{N_b}\sum_{j\in type} P_{RES,ij}^t * n_i * l_i \leqslant \sum_{i=2}^{N_b} P_{D,i}^t \tag{44}$$

Capacitor penetration constraint in network:

$$\sum_{i=2}^{N_b} Q_{cap}^t * m_i * c_i \leqslant \sum_{i=2}^{N_b} Q_{D,i}^t \tag{45}$$

Utility economy constraint:

$$EI \geqslant 1.0 \tag{46}$$

Optimization framework

EI, $Ploss_{avg}$, VSF_{avg}, NSI_{avg} and ACE_{avg} are functions of location, type and size of RESs, and location and size of capacitor bank. The utility want to get the higher values of EI and VSF_{avg}, and lower values of $Ploss_{avg}$, NSI_{avg} and ACE_{avg} simultaneously for achieving improved techno-economic and environmental friendly distribution system. The maximization of EI and VSF_{avg} designates the minimization of $\{-EI\}$ and $\{-VSF_{avg}\}$ respectively. So, the multi-objective optimization problem can be formulated as

$$\min\{\vec{f}(\vec{x})\} \quad s.t. \quad (38) \quad to \quad (46) \tag{47}$$

where $\vec{f}(\vec{x}) = \left[-EI(\vec{x}), Ploss_{avg}(\vec{x}), -VSF_{avg}(\vec{x}), NSI_{avg}(\vec{x}), ACE_{avg}(\vec{x})\right]^T$ is the vector of objective functions and $\vec{x} = [n, l, j, m, c]^T$ is the vector of decision variables. So, the multiple objectives are optimized with respect to the variation of location, type and size of RESs, and location and size of capacitor units in the distribution network. However, the choice of RESs is also dependent on their power injection possibilities. The optimization framework considering intermittent generation of RES units and reactive power support of capacitor banks is shown in Fig. 1.

Application of MOPSO

MOPSO method

PSO is a simple and computationally effective stochastic search technique well suited for complex and nonlinear optimization problems [28]. PSO is a swarm intelligence method for deriving optimal solution, inspired by the social behavior metaphor of lower animals. In PSO, the particles in a swarm 'fly' in a multidimensional problem space to search for possible optimal solution. In each flight particles adjust their position and velocity based on past personal experience and from the success of their peers [29]. The position and velocity modification of the particles can realized through the following expression.

$$\vartheta_{i+1}^d = \varphi\vartheta_i^d + C_1 rand_1^d\left(pbest_i^d - x_i^d\right) + C_2 rand_2^d\left(gbest^d - x_i^d\right) \tag{48}$$

$$x_{i+1}^d = x_i^d + \vartheta_{i+1}^d \tag{49}$$

where φ is the inertia of weight and given by

$$\varphi = \varphi_{\max} - \left(\frac{\varphi_{\max} - \varphi_{\min}}{iter_{\max}}\right) iter \tag{50}$$

Maximum weight, $\varphi_{\max}$ and minimum weight, $\varphi_{\min}$ are set as 0.9 and 0.4 respectively. $iter_{\max}$ and $iter$ are the maximum iteration number and current iteration number. C_1 and C_2 are the acceleration coefficients and considered as 2.0 for both. $rand_1{}^d$ and $rand_2{}^d$ are two uniformly distributed random numbers independently generated within {0, 1} for the dth dimension. The best personal experience is called *pbest* and the swarm's best experience is called *gbest*. After every iteration, particles move toward the potential solution region.

Unlike a unique optimal solution in PSO, a set of alternative solutions known as Pareto optimal solutions or non-dominated solutions is generated by MOPSO. These solutions are optimal in the wider sense that no other solutions in decision space are superior to them when multiple objectives are considered. Non-dominated sorting and crowding distance concepts are incorporated into PSO in order to allow this heuristic to handle problems with several objective functions. The crowding distance is a measure of how close an individual is to its neighbors and can be obtained as follows.

$$I[i]_{distance} = \sum_{m=1}^{N_{obj}} \frac{(I[i+1]\cdot m - I[i-1].m)}{\left(f_m^{\max} - f_m^{\min}\right)} \quad \text{for} \quad i = 2 \quad \text{to} \quad n-1 \tag{51}$$

N_{obj} is the total number of objective function. $I[i]\cdot m$ is the value of the mth objective function of the ith individual in the front level I. The individuals in the boundary (i.e. $I[1]$ & $I[n]$) are assigned with infinite distance [30]. In MOPSO, the swarm is sorted into various non-domination front levels based on non-domination criteria. The individuals that are not dominated by the others form the first front. Since the *pbest* particles are chosen from top rank front levels; the selection pressure drives the swarm towards the true non-dominated solutions over many iteration steps. Randomly chosen non-dominated solution from the less-crowded area in first front level is used as guide (*gbest*) of the whole swarm [31]. So, the diversity of the solution is preserved. Applying the constraint handling technique [32], the solutions violating the constraint are avoided to select *gbest*.

Fuzzy based decision making

After maximum iteration, MOPSO generate a set of non-dominated solutions. Final decision should be determined with higher level of qualitative considerations. Fuzzy rule have capability to synthesize the problem and identify the optimal non-dominated solution [33]. A linear fuzzy membership function is chosen with $f^{\min}$ and $f^{\max}$ in the whole solution space. Fuzzy rule

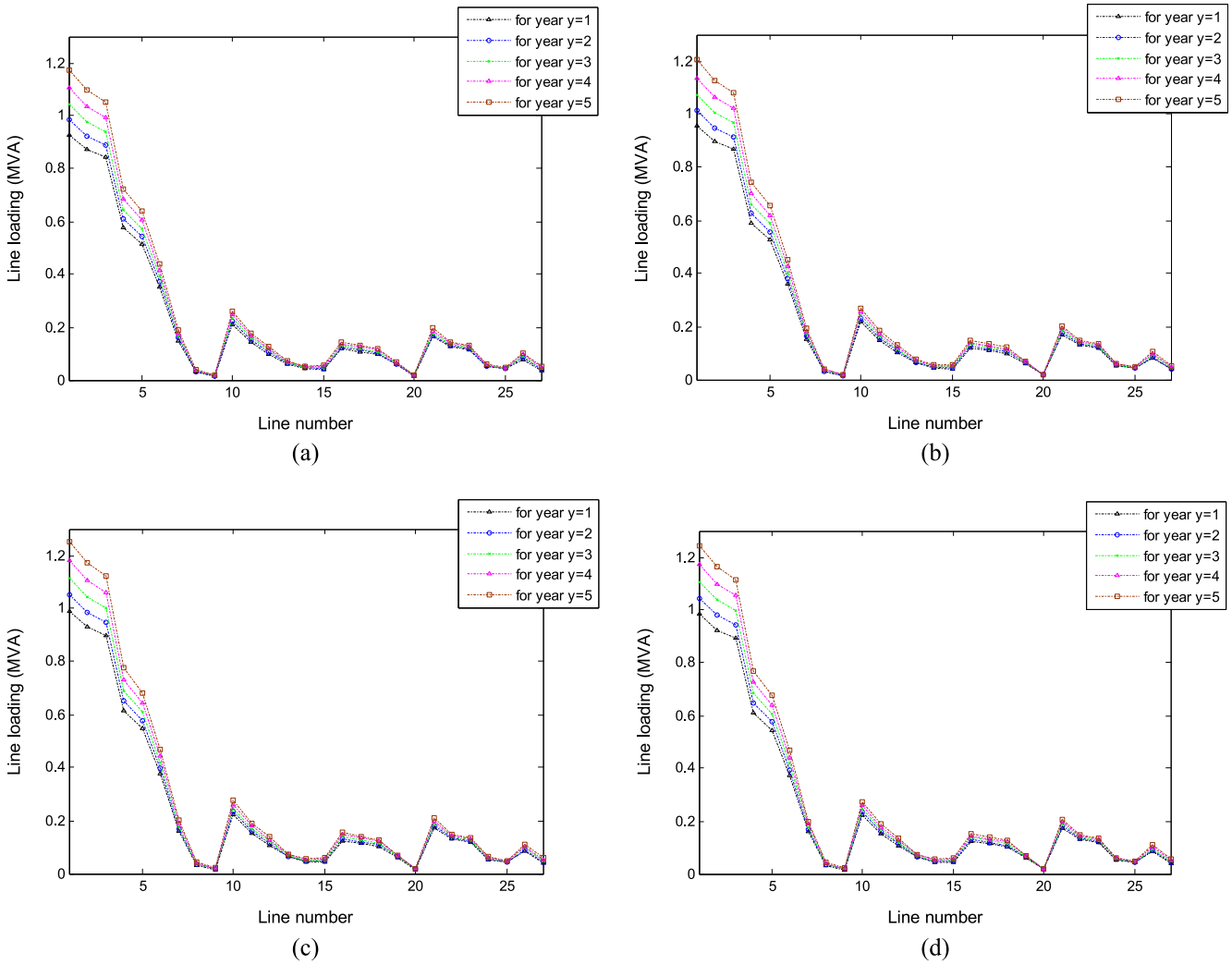

Fig. 10. Impact of load growth on line loading during time period 10.00–11.00 h in (a) Winter. (b) Spring. (c) Summer. (d) Autumn.

can also be formulated with craziness of DISCOs on different objectives. Mathematically fuzzy membership function for each objective in MOPSO can be defined as

$$\psi_i = \begin{cases} 0 & \text{if } f_i \geqslant f_i^{\max} \\ \left(\frac{f_i^{\max} - f_i}{f_i^{\max} - f_i^{\min}}\right) & \text{if } f_i^{\max} > f_i > f_i^{\min} \\ 1 & \text{if } f_i \leqslant f_i^{\min} \end{cases} \quad (52)$$

Overall membership value of any non-dominated solution k is determined by summing of membership values followed by normalization. It can be defined as

$$\psi^k = \frac{\sum_{i=1}^{N_{obj}} \psi_i^k}{\sum_{k=1}^{\mathbb{N}} \sum_{i=1}^{N_{obj}} \psi_i^k} \quad (53)$$

$\mathbb{N}$ is the number of non-dominated solution obtained from MOPSO.

Solution with highest value of ψ^k is selected as best compromising solution.

Solution algorithm

The proposed planning problem is solved using MOPSO technique to generate non-dominated solution with the help of trade-off between multiple objectives. The steps to generate best non-dominated solution and corresponding optimal location, type and size of RESs and, location and size of capacitor bank are as shown in Fig. 2.

Test network and local weather

Network description

Proposed planning method is supposed to be done with an 11 kV, 28-bus rural distribution network [26] situated at Kakdwip region in the state of West Bengal, India. The network is radial in nature with 27 overhead distribution lines as shown in Fig. 3. It is noted from the figure that bus-1 is situated at distribution substation. The line and load data of the test network are provided in Table 1. The power factor of the load is taken as 0.7.

Three types of customer viz. residential, commercial, and industrial customers are present in the network territory. According to types of customers, loads are categorized into residential, commercial and industrial load. Different class of loads exhibit diverse levels of voltage dependencies. Exponent of voltage magnitudes for active and reactive power demand in different class of loads [34] are shown in Table 2. Residential, commercial and industrial customers have different level of power consumption pattern throughout the day as depicted in Fig. 4. Also, there is a seasonal change in power demand trajectories of the customers which can be accessed from the figure.

Local weather

Kakdwip region (21.883°*N*88.183°*E*) has distinct seasonal variation in weather because of its location near to Bay of Bengal and Tropic of Cancer. Four seasons: Summer (May to July), Autumn (August to October), Winter (November to January) and Spring (February to April) is distinctly seen in the region. Each season is being represented by 24 segments, each referring to a particular hourly interval of the entire season. Historical data collected from the site are utilized to calculate mean and standard deviation of solar irradiance and wind speed, and tabulated in Tables 3 and 4 respectively. The data illustrate that wind velocity in winter is usually very low and may be ineffective for wind power generation. On the other hand solar radiation is quite consistent throughout the year in the test region. The location is predominantly characterized by hot and humid weather. The temperature usually varies between 12 and 39 °C in a year. Hourly mean temperatures in four seasons are shown in Fig. 5.

Results and discussion

Proposed planning model has been simulated in MATLAB software on Intel (R) Core (TM) 2 Duo processor with 2.0 GB RAM. The planning period is taken as five years. Newton–Raphson power flow algorithm is used to evaluate line flow and bus voltage magnitudes which accelerate to calculate objective functions. All the buses except the substation bus are considered at candidate locations for RESs and capacitor banks. The maximum number of RESs and capacitor banks at candidate bus is restricted to three, although the developed technique can accept any number of RESs and capacitor units without constraint violation. In fact, maximum installation capacity at a bus location depends on many factors such as network configuration, land availability, policy of DISCOs and social issues. MOPSO algorithm is initialized with 500 particles and 100 iterations. It is to be noted that consideration of lower number of particles may not generate enough number of solutions satisfying constraints at initial stage. However large number of control parameters in the algorithm suffers with time complexity problem. Each particle contains location, type and size (number of units) variables of RESs, and location and size (number of units) variables of capacitor banks. The maximum voltage limit for the buses in the network is taken as 1.05 pu. N_{Dy} is considered as 360. C_{hr} is presumed to be INR 6.5/kW h. IF and IR have considered as 5% and 6% respectively. Carbon-di-oxide emission rate of grid [7] is chosen as 921.25 kg/MW h.

PV array is designed with 600 PV modules which have 132 kW of installed capacity. Specification of PV module is given in Table 5. The WT used in this study have maximum capacity of 250 kW and its power generation pattern depends on the specification tabulated in Table 6. The cost factors of solar and wind power generation technologies [35] are furnished in Table 7. Technical and economic specification of capacitor bank [36] are listed in Table 8.

Table 14
Study on power flow through line-3 (line loading within safe limit: ϒ; line loading violates maximum limit: ×).

	Time segment (h)																
	1	…	9	10	11	12	13	14	15	16	17	18	19	20	21	…	24
Winter	ϒ	…	ϒ	ϒ	ϒ	ϒ	ϒ	ϒ	ϒ	ϒ	ϒ	ϒ	ϒ	ϒ	ϒ	…	ϒ
Spring	ϒ	…	ϒ	ϒ	ϒ	ϒ	ϒ	ϒ	ϒ	ϒ	×	ϒ	ϒ	ϒ	ϒ	…	ϒ
Summer	ϒ	…	ϒ	×	×	×	×	ϒ	×	×	×	ϒ	×	×	ϒ	…	ϒ
Autumn	ϒ	…	ϒ	ϒ	×	×	×	ϒ	ϒ	ϒ	ϒ	ϒ	ϒ	ϒ	ϒ	…	ϒ

Kakdwip is situated in the eastern region of India. The 18th power survey by Central Electricity Authority [37] estimates that APEL in eastern region of India will be increased from 17,482 MW in 2012–13 to 33,747 MW in 2021–22. So nine years cumulative load growth was predicted as 93%. The 17th power survey [38] estimated that compound annual growth rate (CAGR) for residential, commercial and industrial consumers were 17.7%, 5.5% and 9.2% respectively in the period of 2003–04 to 2011–12. In the same time period CAGR for total consumer in the eastern region was considered as 11.4%. Taking into account the similar ratio of load growth in specific consumer to total consumer (2003–04 to 2011–12), CAGR for the residential, commercial and industrial consumers in the study period are calculated as 10.4%, 4.2% and 6.4% respectively.

Optimization results

The set of non-dominated solution generated by MOPSO for mixed RES–capacitor planning is presented in Table 9. It can be observed from the results that no unique solution is there which reflects superiority of all the objectives. So, the best compromised solution is identified utilizing Fuzzy decision tool from the set of non-dominated solution. The obtained optimum solution is marked in Table 9. The location, type and size of RESs, and location and size of capacitor banks correspond to the best non-dominated solution are shown in Table 10.

The technical, economical and environmental aspects of optimum RES–capacitor reinforcement is compared with base network performance scenario in Table 11. It is seen from the table that considerable economical, technical and environmental advantages can be achieved with mixed penetration of RESs and capacitor bank in distribution system. The results indicate that 49.9% lower power losses, 2.2% better voltage stability condition and 8.1% improved network security level can be achieved with proposed planning model. The utility can also make profit of INR 258.7915×10^5 from the project and the total saving of carbon-di-oxide emission in the planning period is 7890 ton.

Efficiency of the distribution system is also investigated employing lone RESs and lone capacitor bank. The simulation results obtained for the case of RESs planning and capacitor bank planning are presented in Tables A1 and A2 respectively in Appendix. The best non-dominated solution obtained for the three planning model (i.e. with RES–capacitor, with RESs only and with capacitor only) are compared in Table 12. The results indicate that application of capacitor provides moderate techno-economic prosperity and marginal emission reduction. Although *EI* is very high, the profit of utility is calculated as INR 35.1967×10^5. As the capacitor penetration creates very little impact on grid power consumption, carbon-di-oxide emission is mostly unaffected throughout the year. On the other hand application of RESs can result drastic diminution in carbon-di-oxide emission with considerable profit. The profit of the utility is calculated as INR 233.5575×10^5. However maximum technical, economic and environmental benefit is obtained for the case of mix penetration. So, it can be confirmed that application of RES–capacitor is more effectual over solitary RES and capacitor reinforcement.

Voltage profile at low voltage points can also be improved substantially utilizing mixed RES–capacitor planning. Fig. 6 shows that minimum bus voltage value has been raised at appreciably higher voltage level. There is also sufficient loading release at the lines with heavy power flow. The comparative study at different penetration case for the line with maximum burden throughout the year is shown in Fig. 7.

Effect of load growth

Peak electric demand at the load buses becomes progressively higher due to annual load growth. Fig. 8 illustrates the modified peak load in the consecutive years considering specified CAGR. The growing load demand in distribution system has significant impact on the performance of the distribution network. The comparative study presented in Table 13 indicates that network performance would become poor because of load growth. The analyses depict that load growth causes 29.9% increased power losses, 0.8% reduction of voltage stability and 12.7% drop in network security situation respectively. Also the utility have to bear 3665 ton more carbon-di-oxide emission in five years to meet the increased demand due to load growth.

Load growth causes lower voltage profile at distribution buses as observed in Fig. 9. To supply the increased customer demand power flowing through the distribution lines become higher as shown in Fig. 10. Importantly line power flow may exceed their critical loading capacity. After hour to hour investigation in the total planning horizon it is seen that in the final year of planning period line-3 violates its line loading limit in some time segment as given in Table 14. Throughout the winter season power flow in all lines are found within the safe limit. However, application of RES and capacitor units in the network can alleviate power flow in line-3. Thus reliability of power supply is restored and substantial cost for network upgradation is saved.

Conclusion

This paper has presented a multi-objective optimization model for mix penetration of PV array, wind turbine and capacitor bank in electrical distribution network. MOPSO algorithm is employed to generate set of potential solutions after considering all possible trade-offs between technical, economic and environmental objectives. Utilizing fuzzy decision criteria the proposed solution strategy confirms to identify the best non-dominated solution satisfying bus voltage, RES penetration, capacitor penetration and line capacity constraints. Optimization result indicates that significant reduction in pollutant emission and effective improvement in network power loss, voltage stability and network security condition can be attained with considerable economic benefit. The detrimental effects of load growth can be overcome with combined RES and capacitor bank allocation in the network. Voltage magnitude of buses is improved significantly and line loadings are relieved appreciably after allocation of RESs and capacitor banks. Thus the sustainability of the network is facilitated. The study also reveals that mix penetration of RESs and capacitor creates multitude benefit over solitary RESs and capacitor allocation. So, the utility can supply higher quality and reliable power to the customers with the proposed RES–capacitor planning approach. Moreover the utility would be benefited with significant cash inflow from the project. The work of this paper will be specifically useful to electric power utilities striving to survive in the competitive electricity market.

Acknowledgement

The authors would like to thank the West Bengal Renewable Energy Development Agency for their support to arrange resource data.

Appendix A

See Tables A1 and A2.

Table A1
Non-dominated solutions obtained for the planning model of distribution system with RESs.

Non-dominated solution	$-EI$	$Ploss_{avg}$	$-VSF_{avg}$	NSI_{avg}	ACE_{avg}
1	−1.7100	0.0349	−0.9503	0.3713	4233
2	−1.7083	0.0351	−0.9518	0.3872	4242
3	−1.7136	0.0345	−0.9508	0.3644	4233
4	−1.7809	0.0346	−0.9508	0.3694	4267
5	−1.5988	0.0415	−0.9427	0.3797	5358
6	−1.5990	0.0415	−0.9427	0.3791	5357
7	−1.6959	0.0403	−0.9438	0.3802	4993
8	−1.6202	0.0408	−0.9433	0.3815	5356
9	−1.7436	0.0378	−0.9461	0.3717	4807
10	−1.7699	0.0358	−0.9489	0.3745	4626
11	−1.6119	0.0383	−0.9463	0.3766	4958
12	−1.6795	0.0362	−0.9483	0.3749	4592
13	−1.7718	0.0356	−0.9495	0.3782	4448
14	−1.7572	0.0368	−0.9476	0.3721	4807
15	−1.7787	0.0348	−0.9508	0.3692	4269
16	−1.6862	0.0367	−0.9478	0.3740	4413
17	−1.5845	0.0401	−0.9447	0.3833	4964
18	−1.6863	0.0367	−0.9487	0.3827	4418
19	−1.6032	0.0389	−0.9464	0.3838	4962
20	−1.7742	0.0354	−0.9496	0.3664	4448
21	−1.6616	0.0379	−0.9469	0.3759	4597
22	−1.7716	0.0356	−0.9488	0.3721	4445
23	−1.7346	0.0379	−0.9459	0.3770	4987
24	−1.7766	0.0351	−0.9499	0.3720	4267
25	−1.7658	0.0362	−0.9480	0.3761	4625
26	−1.6988	0.0353	−0.9497	0.3687	4444
27	−1.7158	0.0391	−0.9448	0.3778	4990
28	−1.7568	0.0368	−0.9475	0.3730	4807
29	−1.6210	0.0408	−0.9434	0.3806	5355
30	−1.6202	0.0408	−0.9433	0.3815	5355
31	−1.7111	0.0348	−0.9512	0.3773	4237
32	−1.6998	0.0352	−0.9505	0.3710	4417
33	−1.6899	0.0363	−0.9488	0.3758	4416
34	−1.7729	0.0355	−0.9493	0.3701	4267
35	−1.7117	0.0347	−0.9509	0.3775	4234
36	−1.6768	0.0365	−0.9481	0.3724	4593
37	−1.7655	0.0362	−0.9480	0.3700	4625
38	−1.6618	0.0379	−0.9467	0.3764	4597
39	−1.5988	0.0415	−0.9427	0.3797	5358
40	−1.7241	0.0386	−0.9453	0.3737	4988
41	−1.6805	0.0361	−0.9490	0.3719	4595
42	−1.7256	0.0385	−0.9453	0.3797	4988
43	−1.7238	0.0386	−0.9455	0.3739	4989
44	−1.6028	0.0390	−0.9453	0.3759	4958
45	−1.7228	0.0387	−0.9452	0.3761	4988
46	−1.7319	0.0381	−0.9460	0.3760	4988
47	−1.6883	0.0365	−0.9482	0.3739	4414
48	−1.7068	0.0353	−0.9499	0.3723	4234
49	−1.6933	0.0359	−0.9497	0.3770	4417
50	−1.6787	0.0363	−0.9489	0.3763	4596
51	−1.7122	0.0347	−0.9507	0.3759	4233
52	−1.7710	0.0357	−0.9491	0.3720	4267

The 'gray shaded' row represents the best solution in the total solution set.

Table A2
Non-dominated solutions obtained for the planning model of distribution system with capacitor bank.

Non-dominated solution	$-EI$	$Ploss_{avg}$	$-VSF_{avg}$	NSI_{avg}	ACE_{avg}
1	−72.1900	0.0320	−0.9537	0.4004	5726
2	−82.0311	0.0304	−0.9536	0.3650	5712
3	−77.5144	0.0312	−0.9513	0.3737	5707
4	−64.7914	0.0386	−0.9442	0.3805	5733
5	−69.4864	0.0324	−0.9537	0.4267	5727
6	−67.2537	0.0328	−0.9523	0.4081	5724
7	−75.4394	0.0315	−0.9536	0.3932	5720
8	−96.2067	0.0360	−0.9464	0.3746	5723
9	−72.0680	0.0320	−0.9521	0.3905	5718
10	−49.2507	0.0357	−0.9487	0.4015	5730
11	−71.2730	0.0380	−0.9447	0.3853	5731
12	−51.9768	0.0353	−0.9486	0.3857	5727
13	−74.9882	0.0315	−0.9536	0.3828	5722
14	−80.8356	0.0306	−0.9531	0.3654	5712
15	−78.1485	0.0311	−0.9518	0.3694	5709
16	−54.7916	0.0349	−0.9478	0.3776	5720
17	−80.4494	0.0307	−0.9531	0.3774	5712
18	−77.6865	0.0311	−0.9514	0.3719	5707
19	−78.1197	0.0310	−0.9534	0.3708	5717
20	−74.4660	0.0316	−0.9520	0.3782	5714
21	−54.1487	0.0350	−0.9484	0.3783	5723

The 'gray shaded' row represents the best solution in the total solution set.

References

[1] Kaldellis JK, Zafirakis D. The wind energy revolution: a short overview of a long history. Renew Energy 2011;36:1887–901.
[2] Celik AN. Optimization and techno-economic analysis of autonomous photovoltaic–wind hybrid energy systems in comparison to single photovoltaic and wind systems. Energy Convers Manage 2002;43:2453–68.
[3] Zhou W, Lou C, Li Z, Lu L, Yang H. Current status of research on optimum sizing of standalone hybrid solar–wind power generation systems. Appl Energy 2010;87:380–9.
[4] Wang L, Singh C. Multicriteria design of hybrid power generation systems based on a modified particle swarm optimization algorithm. IEEE Trans Energy Convers 2009;24:163–72.
[5] Bayod-Rujula AA, Haro-Larrode ME, Martinez-Gracia A. Sizing criteria of hybrid photovoltaic–wind systems with battery storage and self consumption considering interaction with the grid. Sol Energy 2013;98:582–91.
[6] Yanine FF, Sauma EE. Review of grid-tie micro generation systems without energy storage: towards a new approach to sustainable hybrid energy systems linked to energy efficiency. Renew Sustain Energy Rev 2013;26:60–95.
[7] Nasiraghdam H, Jadid S. Optimal hybrid PV/WT/FC sizing and distribution system reconfiguration using multi-objective artificial bee colony (MOABC) algorithm. Sol Energy 2012;86:3057–71.
[8] Khatod DK, Pant V, Sharma J. Evolutionary programming based optimal placement of renewable distributed generators. IEEE Trans Power Syst 2013;28:683–95.
[9] Alsayed M, Cacciato M, Scarcella G, Scelba G. Multicriteria optimal sizing of photovoltaic–wind turbine grid connected system. IEEE Trans Energy Convers 2013;28:370–9.
[10] Alsayed M, Cacciato M, Scarcella G, Scelba G. Design of hybrid power generation system based on multi criteria decision analysis. Sol Energy 2014;105:548–60.
[11] Raju MR, Murthy KVSR, Ravindra K. Direct search algorithm for capacitive compensation in radial distribution systems. Elect Power Energy Syst 2012;42:24–30.
[12] Tabatabaei SM, Vahidi B. Bacterial foraging solution based fuzzy logic decision for optimal capacitor allocation in radial distribution system. Elect Power Syst Res 2011;81:1045–50.
[13] Sultana S, Roy PK. Optimal capacitor placement in radial distribution systems using teaching learning based optimization. Elect Power Energy Syst 2014;54:387–98.
[14] Naik SG, Kathod DK, Sharma MP. Optimal allocation of DG and capacitor for real power loss minimization in distribution networks. Elect Power Energy Syst 2013;53:967–73.
[15] Sajjadi SM, Haghifam M, Salehi J. Simultaneous placement of distributed generation and capacitors in distribution networks considering voltage stability index. Electr Power Energy Syst 2013;46:366–75.

[16] Moradi MH, Zeinalzadeh A, Mohhamadi Y, Abedini M. An efficient hybrid method for solving the optimal sitting and sizing problem of DG and shunt capacitor banks simultaneously based on imperialist competitive algorithm and genetic algorithm. Electr Power Energy Syst 2014;54:101–11.
[17] Atwa YM, El-Saadany EF, Salama MMA, Seethapathy R. Optimal renewable resources mix for distribution system energy loss minimization. IEEE Trans Power Syst 2010;25:360–70.
[18] Karaki SH, Chedid RB, Ramadan R. Probabilistic performance assessment of autonomous solar–wind energy conversion systems. IEEE Trans Energy Convers 1999;14:766–72.
[19] Hung DQ, Mithulananthan N, Bansal RC. Integrating of PV and BES units in commercial distribution systems considering energy loss and voltage stability. Appl Energy 2014;113:1162–70.
[20] Hongxing Y, Wei Z, Chengzhi L. Optimal design and techno-economic analysis of a hybrid solar–wind power generation system. Appl Energy 2009;86:163–9.
[21] Aman MM, Jasmon GB, Mokhlis H, Bakar AHA. Optimal placement and sizing of a DG based on a new power stability index and line losses. Electr Power Energy Syst 2012;43:1296–304.
[22] Kashem MA, Ganapathy V, Jasmon GB. Network reconfiguration for enhancement of voltage stability in distribution networks. IEE Proc Gener Transm Distrib 2000;147:171–5.
[23] Shin JR, Kim BS, Park JB, Lee KY. A new optimal routing algorithm for loss minimization and voltage stability improvement in radial power systems. IEEE Trans Power Syst 2007;22:648–57.
[24] Kayal P, Chanda CK. Placement of wind and solar based DGs in distribution system for power loss minimization and voltage stability improvement. Electr Power Energy Syst 2013;53:795–809.
[25] Kayal P, Chanda CK. Optimal mix of solar and wind distributed generations considering performance improvement of electrical distribution network. Renew Energy 2015;72:173–86.
[26] Singh RK, Goswami SK. Multi-objective optimization of distributed generation planning using impact indices and trade-off technique. Electr Power Compon Syst 2011;39:1175–90.
[27] IEA Report. World energy outlook 2014: executive summary. International Energy Agency; 2014. p. 1–7.
[28] Coelho LS, Guerra FA, Liete J. Multiobjective exponential particle swarm optimization approach applied to hysteresis parameters estimation. IEEE Trans Magn 2012;48:283–6.
[29] Kennedy J, Eberhart RC. Particle swarm optimization. In: Proceedings of IEEE international conference on neural network; 1995. p. 1942–8.
[30] Deb K, Pratap A, Agarwal S, Meyarivan T. A fast and elitist multi-objective genetic algorithm: NSGA-II. IEEE Trans Evol Comput 2002;6:182–97.
[31] Raquel CR, Naval PC. An effective use of crowding distance in multi objective particle swarm optimization. In: Proceedings of genetic and evolutionary computation conference; 2005. p. 257–264.
[32] Coello CAC, Pulido GT, Lechuga MS. Handling multiple objectives with particle swarm optimization. IEEE Trans Evol Comput 2004;8:256–79.
[33] Hazra J, Sinha AK. A multi-objective optimal power flow using particle swarm optimization. Eur Trans Electr Power 2010;21:1028–45.
[34] Singh D, Misra RK, Singh D. Effect of load models in distributed generation planning. IEEE Trans Power Syst 2007;22:2204–12.
[35] Shrimali G, Srinivasan S, Goel S, Trivedi S, Nelson D. Reaching India's renewable energy targets cost-effectively. CPI-ISB series; April 2015.
[36] Gnanasekaran N, Chandramohan S, Sudhakar TD, Kumar PS. Maximum cost saving approach for optimal capacitor placement in radial distribution systems using modified ABC algorithm. Electr Eng Infor 2015;7:665–78.
[37] Report on Eighteenth Electric power survey of India. Central Electricity Authority, India; 2011.
[38] Report on Seventeenth Electric power survey of India. Central Electricity Authority, India; 2007.